Ssdp1 regulates head morphogenesis of mouse embryos by activating the Lim1-Ldb1 complex

Noriyuki Nishioka[1,2], Seiichi Nagano[3], Rika Nakayama[4], Hiroshi Kiyonari[4], Takashi Ijiri[5], Kenichiro Taniguchi[6], William Shawlot[6], Yoshihide Hayashizaki[7], Heiner Westphal[8], Richard R. Behringer[9], Yoichi Matsuda[5,10], Saburo Sakoda[3], Hisato Kondoh[2] and Hiroshi Sasaki[1,*]

[1]Laboratory for Embryonic Induction, RIKEN Center for Developmental Biology, 2-2-3 Minatojima-minamimachi, Chuo-ku, Kobe, Hyogo 650-0047, Japan
[2]Graduate School of Frontier Biosciences, Osaka University, 1-3 Yamadaoka, Suita, Osaka 565-0871, Japan
[3]Department of Neurology, Graduate School of Medicine, Osaka University, D-4, 2-2 Yamadaoka, Suita, Osaka 565-0871, Japan
[4]Laboratory for Animal Resources and Genetic Engineering (LARGE), RIKEN Center for Developmental Biology, 2-2-3 Minatojima-minamimachi, Chuo-ku, Kobe, Hyogo 650-0047, Japan
[5]Division of Bioscience, Graduate School of Environmental Earth Science, Hokkaido University, North 10 West 8, Sapporo 060-0810, Japan
[6]Department of Genetics, Cell Biology, and Development, University of Minnesota, Minneapolis, MN 55455, USA
[7]Laboratory for Genome Exploration Research Group, Genomic Sciences Center, RIKEN, Yokohama, Kanagawa 230-0045, Japan
[8]Laboratory of Mammalian Genes and Development, National Institute of Child Health and Human Development, National Institutes of Health, Bethesda, MD 20892, USA
[9]Department of Molecular Genetics, The University of Texas M. D. Anderson Cancer Center, Huston, TX 77030, USA
[10]Center for Advanced Science and Technology, Hokkaido University, North 10 West 8, Sapporo 060-0810, Japan
*Author for correspondence (e-mail: sasaki@cdb.riken.jp)

Accepted 1 April 2005

Development 132, 2535-2546
Published by The Company of Biologists 2005
doi:10.1242/dev.01844

Development

Summary

The transcriptional activity of LIM-homeodomain (LIM-HD) proteins is regulated by their interactions with various factors that bind to the LIM domain. We show that reduced expression of single-stranded DNA-binding protein 1 (*Ssdp1*), which encodes a co-factor of LIM domain interacting protein 1 (Ldb1), in the mouse mutant *headshrinker* (*hsk*) disrupts anterior head development by partially mimicking *Lim1* mutants. Although the anterior visceral endoderm and the anterior definitive endoderm, which together comprise the head organizer, were able to form normally in *Ssdp1*$^{hsk/hsk}$ mutants, development of the prechordal plate was compromised. Head development is partially initiated in *Ssdp1*$^{hsk/hsk}$ mutants, but neuroectoderm tissue anterior to the midbrain-hindbrain boundary is lost, without a concomitant increase in apoptosis. Cell proliferation is globally reduced in *Ssdp1*$^{hsk/hsk}$ mutants, and approximately half also exhibit smaller body size, similar to the phenotype observed in *Lim1* and *Ldb1* mutants. We also show that Ssdp1 contains an activation domain and is able to enhance transcriptional activation through a Lim1-Ldb1 complex in transfected cells, and that *Ssdp1* interacts genetically with *Lim1* and *Ldb1* in both head development and body growth. These results suggest that Ssdp1 regulates the development of late head organizer tissues and body growth by functioning as an essential activator component of a Lim1 complex through interaction with Ldb1.

Key words: Ssdp1, Head organizer, Prechordal plate, Headshrinker, Lim1, Ldb1, Cell proliferation, Mouse

Introduction

Members of the LIM-homeodomain (LIM-HD) family of transcription factors play important roles in various aspects of both vertebrate and invertebrate development (Bach, 2000; Bachy et al., 2002; Hobert and Westphal, 2000). One such factor, Lim1 (Lhx1), is required during early stages of vertebrate development to establish anterior patterning (Shawlot and Behringer, 1995). *Lim1*-deficient mouse embryos fail to establish the head organizer, the signaling center that initiates and promotes the head differentiation program in naïve ectoderm. In the mouse embryo, head organizer activity resides in two distinct regions, the anterior visceral endoderm (AVE) and the anterior primitive streak. The AVE first confers anterior character to the overlying anterior epiblast at egg cylinder stage (Beddington and Robertson, 1999; Tam and Steiner, 1999). Following the onset of gastrulation, the anterior definitive endoderm (ADE) and the prechordal plate, which arise from the anterior primitive streak and constitute the anterior region of the axial mesendoderm (AME), intercalate into the outer visceral endoderm layer and displace the AVE, inducing and maintaining anterior neural character in the overlying epiblast. *Lim1* mutant embryos fail to specify the AVE and the anterior AME, resulting in the loss of head structures anterior to rhombomere 3 (Shawlot and Behringer, 1995; Shawlot et al., 1999). In addition, *Lim1* mutants show defects in body axis extension because of impaired cell movements during gastrulation (Hukriede et al., 2003; Tam et al., 2004).

LIM-HD transcription factors contain two LIM domains that regulate their activity. LIM domain-binding proteins, which include Ldb1 (NLI/CLIM2) and Ldb2 (CLIM1) in vertebrates and Chip (dLDB) in *Drosophila*, bind to LIM-HD transcription factors (Agulnick et al., 1996; Jurata et al., 1996) and promote the formation of $(\text{LIM-HD})_2$-$(\text{Ldb1})_2$ tetramers through their dimerization domain (Jurata et al., 1998). Formation of this tetrameric complex is required for the transcriptional activator function of LIM-HD proteins in vivo (Hiratani et al., 2003; Milan and Cohen, 1999; Thaler et al., 2002; van Meyel et al., 1999). In addition, it has recently been shown that the single-stranded DNA-binding protein (Ssdp) proteins (Bayarsaihan et al., 1998) bind to Ldb1/Chip (Chen et al., 2002; van Meyel et al., 2003). In *Drosophila*, a functional complex of Ssdp, Chip and the LIM-HD protein Apterous plays an important role in wing development (Chen et al., 2002; van Meyel et al., 2003). Although a similar mechanism was suggested for vertebrate Ssdp proteins (Chen et al., 2002), their roles in the developmental regulation of LIM-HD proteins in vivo are unknown.

In this study, we generated a novel mouse mutant, *headshrinker* (*hsk*), by transgene insertion. At birth, *hsk* mutants lacked head structures anterior to the ear, a phenotype that is reminiscent of head organizer defects. Mapping of the transgene insertion revealed an intronic disruption of the *Ssdp1* locus. Transgenic expression of exogenous *Ssdp1* was able to rescue the *hsk* mutants, indicating that disruption of *Ssdp1* is responsible for the *hsk* phenotype. The head organizer developed normally in $Ssdp1^{hsk/hsk}$ mutants at early stages, but later development was compromised. In addition to exhibiting severe anterior truncations, *Ssdp1* mutants also showed reduced cell proliferation, with half of the mutants exhibiting smaller body size than their wild-type littermates. Furthermore, we show that Ssdp1 contains an activation domain and is able to enhance transcriptional activation by the Lim1-Ldb1 complex in a dose-dependent manner in transfected cells. Finally, we show that *Ssdp1* interacts genetically with *Lim1* and *Ldb1* in both head development and body growth. Together, these data indicate that Ssdp1 functions as an activator component of a Lim1-Ldb1-Ssdp1 complex that plays an essential role in head organizer development and body growth in mouse embryos.

Materials and methods

Mouse lines

Transgenic mice were produced by pronuclear injection of transgene DNA into C57BL/6×C3H/He F2 fertilized eggs (Hogan et al., 1994). The *headshrinker* mutant line was generated in the process of producing transgenic mouse lines harboring a human copper-zinc superoxide dismutase 1 (*SOD1*) transgene, which consists of an 11 kb genomic DNA fragment with a mutant form of the *SOD1* gene that has a 2 bp deletion (Pramatarova et al., 1994). The *headshrinker* line was maintained by crosses with C57BL/6×C3H/He F1 mice. For the rescue experiments, the *Ssdp1* transgene was created by cloning the full-length mouse *Ssdp1* cDNA (Okazaki et al., 2002) into the pCAGGS vector (Niwa et al., 1991). For genetic interaction studies, $Lim1^{+/-}$ mutants (Shawlot and Behringer, 1995) and $Ldb1^{+/-}$ mutants (Mukhopadhyay et al., 2003) were crossed with $Ssdp1^{+/hsk}$ mutants.

Identification of transgene insertion site

The sequences flanking the transgene insertion site were amplified using the LA-PCR in vitro Cloning Kit (Takara). Specific primers were designed for the 5′ end of the *SOD1* transgene: S1 (5′-GTCATTAGTTATGACTGAGTTTGGCCACAGCG-3′), S2 (5′-TGAGGGTATAGAAAGACGCTACACCTCAATCC-3′).

Two *Bam*HI genomic DNA fragments (1.2 kb and 1.6 kb) were used for sequence analysis.

Genotype determination

Embryos were genotyped by PCR using primer P2 (5′-GATGAAATGCTGGACTGAGC-3′) and primer P3 (5′-TGCTTGGTTACCGTGTTAGC-3′) for the wild-type allele (400 bp), and primer P1 (5′-GTTACTCAGCAATTGGGACGCC-3′) and P2 for the mutant allele (510 bp). The positions of the primers are indicated in Fig. 2E. DNA samples of adults and embryos older than E7.5 were prepared from ear punches and yolk sacs, respectively. PCR products were amplified for 30 cycles of 95°C for 30 seconds, 60°C for 1 minute and 72°C for 1 minute. The genotypes of embryos younger than E7.25 were determined following in situ hybridization analysis. The genotypes of *Lim1* and *Ldb1* mutants were determined as previously described (Mukhopadhyay et al., 2003; Shawlot and Behringer, 1995).

Preparation of skeletal specimens

The cartilage and bone of P0 neonates were stained with Alcian Blue and Alizarin Red, respectively, as previously described (Hogan et al., 1994).

Chromosomal FISH

Preparation of chromosome spreads and FISH were performed as previously described (Matsuda and Chapman, 1995). The 11 kb *SOD1* transgene was labeled by nick translation with biotin 16-dUTP (Roche). The hybridized probes were reacted with a goat anti-biotin antibody (Vector Laboratories) and then stained with fluorescein-conjugated donkey anti-goat IgG (Nordic Immunology).

Northern blot analysis

Northern blot analysis of E9.5 total RNA isolated by an RNeasy Mini Kit (Qiagen) was performed using ULTRAhyb™ (Ambion) following the manufacturer's instructions. Radioactive signal was measured with a BAS2500 bio-imaging analyzer (Fuji Film) and normalized using β-actin as a reference.

RNA quantitation by RT-PCR

Total RNA (1 μg) was used for cDNA synthesis with Ready-To-Go You Prime First Strand Beads (Amersham), followed by quantitative PCR using SYBR Premix Ex Tag (Takara) and ABI PRISM 7900HT (Perkin Elmer). The PCR primers used for *Ssdp1* were 5′-atggagccccaccacatgaatg-3′ and 5′-ctggaaggagtggaggaagttc-3′; primers for β-actin were 5′-tgtatgcctctggtcgtaccacag-3′ and 5′-gatgtcacgcacgatttccctctc-3′. The signals were normalized using β-actin as a reference.

In situ hybridization

Mouse embryos were staged by morphology (Downs and Davies, 1993). In situ hybridization was performed according to standard procedures (Henrique et al., 1995; Sasaki and Hogan, 1994; Wilkinson, 1992). The following probes were used: *Foxg1* (Hatini et al., 1994), *Cerl* (Belo et al., 1997), *Dkk1* (Glinka et al., 1998), *En2* (Joyner and Martin, 1987), *Fgf8* (Crossley and Martin, 1995), *Foxa2* (Sasaki and Hogan, 1994), *Foxd4* (Kaestner et al., 1995), *Gsc* (Blum et al., 1992), *Hhex* (Thomas et al., 1998), *Krox20* (Nieto et al., 1991), *Lefty1* (Meno et al., 1997), *Lim1* (Barnes et al., 1994), *Otx2* (Ang et al., 1994), *Pax6* (Stoykova and Gruss, 1994), *Six3* (Oliver et al., 1995), *Uncx4.1* (Mansouri et al., 1997) and *Wnt1* (Parr et al., 1993). For *Ssdp1*, a 343 bp 3′UTR fragment of the *Ssdp1* cDNA (nucleotides 1534-1876, Accession Number AK011853) was used.

Transfection assay

The transfection of P19 cells with plasmid DNA was performed using the FuGENE6 Transfection Reagent (Roche). Briefly, cells were transfected with 0.4 μg reporter plasmid, 0.4 μg effector plasmids and 0.1 μg pCS2-c-β-gal (Turner and Weintraub, 1994). pG4-tk-Luc (Sasaki et al., 1999) and –492gsc/Luc (Mochizuki et al., 2000) were used as reporter constructs. pCMV-Gal4-mSsdp1, pCS2-Xlim1, pCS2-Xldb1 (Mochizuki et al., 2000) and pCS2-mSsdp1 were used as effectors. mSsdp1 constructs were created by cloning the coding region of mouse *Ssdp1* cDNA into the appropriate vectors. The amount of effector plasmid used was adjusted to 0.4 μg by the addition of pCS2.

Detection of apoptosis and cell proliferation

Detection of apoptotic cells by the TUNEL method and of proliferating cells using anti-mouse PCNA mouse monoclonal antibody (Santa Cruz) was performed as previously described (Kiso et al., 2001).

Results

headshrinker, a novel mouse mutant

While constructing a mouse model of human familial amyotrophic lateral sclerosis, we generated several transgenic mouse lines. All the transgenic mice were normal up to 1 year of age, indicating that the expression of the transgene did not disturb embryonic development. However, when we intercrossed these transgenic mice, one line produced neonates that lacked head structures anterior to the ear (Fig. 1B). Skeletal staining of the these mutants revealed that skull derivatives posterior to and including the supraoccipital bone developed normally, but the bone anterior to this point was abnormal and unidentifiable (Fig. 1D,D′). Based on the severe head truncation at birth and the developmental defects that led to it, we named this mutant *headshrinker* (*hsk*). In addition to exhibiting truncation of anterior skull bones, some homozygous mutants also showed mild skeletal defects in other body parts, including anteroposterior dislocation of the left and right halves of the sternum (Fig. 1F, asterisks), asymmetrical attachment of ribs to the sternum (Fig. 1F, arrowheads), reduction of sternebra number, bifurcation and/or fusion of ribs (Fig. 1H, arrowheads), absence/reduction or lateral splitting of the vertebral body, and a shortened tail (Fig. 1H; data not shown). The gross morphology of the internal organs of the *hsk* homozygous neonates was normal (data not shown).

hsk mutant embryos were morphologically indistinguishable

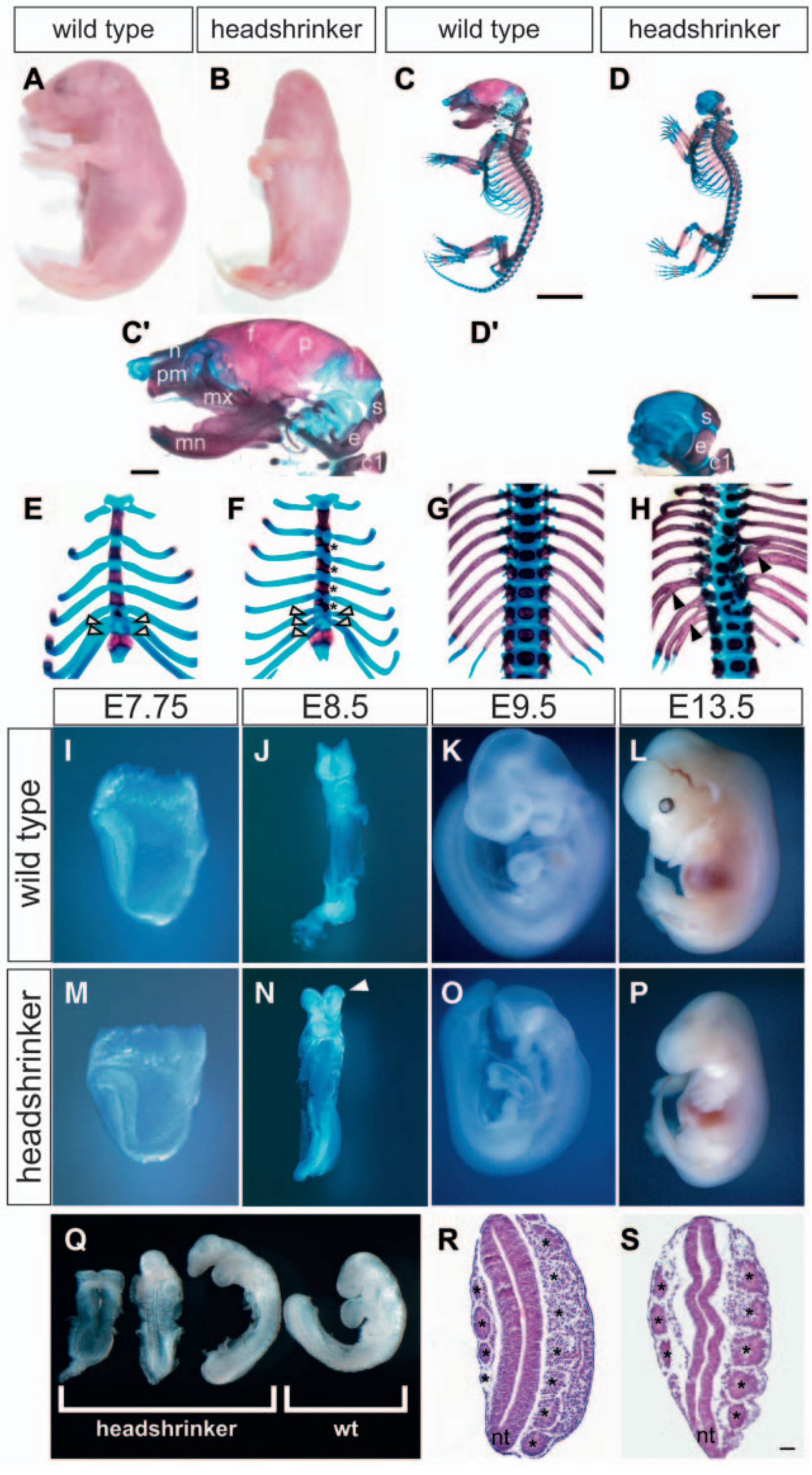

Fig. 1. Gross phenotype of *headshrinker* mutants. (A-H) External views (A,B) and skeletal specimens (C-H) of wild-type (A,C,E,G) and *headshrinker* (*hsk*) mutant (B,D,F,H) P0 neonates. Higher magnification views of the head region of C and D (C′,D′), sternum (E,F) and vertebral bones (G,H). Arrowheads and asterisks in E,F indicate asymmetrical attachment of ribs to the sternum, and anteroposterior dislocation of the sternum, respectively; arrowheads in H indicate bifurcation and/or fusion of ribs. (I-P) The external morphologies of wild-type (I-L) and *hsk* mutant embryos (M-P). The arrowhead in N indicates the abnormality in the anterior neural folds. (Q) Phenotypic variability of *hsk* mutants. Sections of wild-type (R) and *hsk* mutant (S) embryos; asterisks indicate somites. c1, atlas; e, exoccipital bone; f, frontal bone; i, interparietal bone; mn, mandible; mx, maxilla; n, nasal bone; nt, neural tube; p, parietal bone; pm, premaxilla; s, supraoccipital bone. Scale bar: 5 mm in C,D; 1 mm in C′,D′; and 20 μm in R,S.

from wild-type embryos until E7.75 (Fig. 1M). However, although in wild-type embryos the neural plate folded dorsally to form brain vesicles at E8.5, in mutant embryos the head neural plate remained flat (arrow in Fig. 1N). After E9.5, the absence of anterior head structures in *hsk* mutants became evident (Fig. 1O,P). While Mendelian ratios were maintained up to E10.5, the survival ratio for homozygotes declined from E11.5 onwards. The recovery of homozygous animals at birth was 3.4% of total progeny. Approximately half of the mutant embryos were significantly smaller at E9.0 than their wild-type littermates (Fig. 1Q). In addition, the neural tube was thin and kinked, and somites were small and irregular or not formed in some cases (data not shown). Because the head defects were completely penetrant, we focused most of our analysis on this aspect of the mutant phenotype, and selected embryos whose defects were restricted to the head region after E8.5.

Expression of *Ssdp1* was reduced in the *headshrinker* mutant

To identify the gene responsible for the defects observed in *hsk* mutants, we mapped the transgene insertion site. Fluorescence in situ hybridization (FISH) localized the transgene to a single

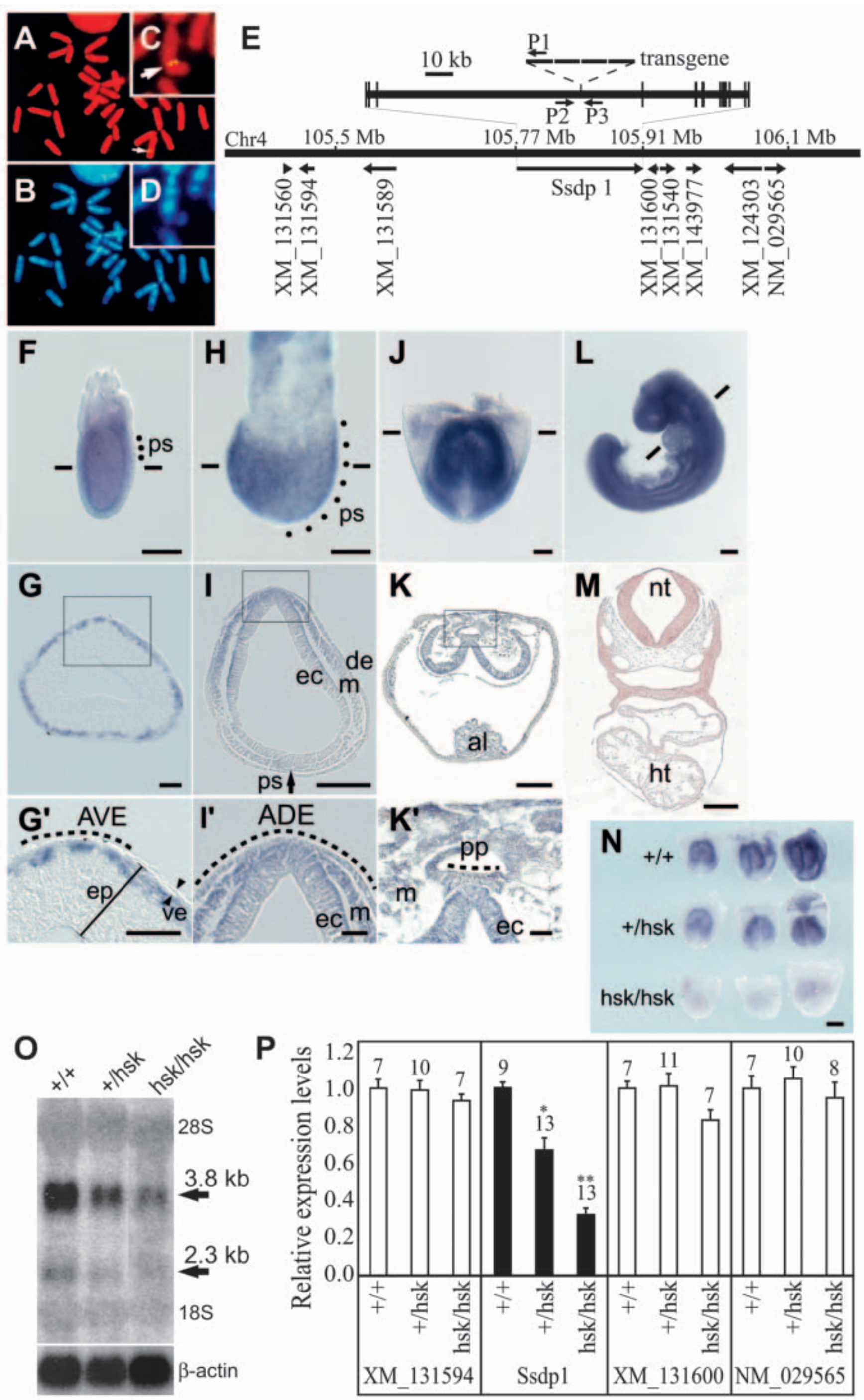

Fig. 2. Identification of the transgene insertion site in *headshrinker* mutants. (A,C) Chromosomal FISH showing the single transgene insertion site at Chr4 C5-C6 (arrow). (B,D) Hoechst 33258 staining of the chromosomes shown in A and C. (C,D) Close up of the transgene insertion site. (E) A physical map of the area surrounding the transgene insertion site. The long horizontal bar at the center represents Chr4, and the positions along the chromosome are given in Mb above the bar. The short arrows below the bar and the numbers indicate the positions of genes and their accession numbers, respectively. The upper bar marked with thinner vertical lines shows the detailed structure of the *Ssdp1* gene. The vertical lines represent exons. Four copies of the transgenes were inserted in the fourth intron of *Ssdp1*. P1, P2 and P3 indicate the positions of the PCR primers used for genotyping. (F,H,J,L) Whole-mount in situ hybridization of *Ssdp1*. Left side view of ES stage (F), LB stage (H), E9.0 (L) and frontal view of E8.0 (J) embryos. (G,I,K) Transverse sections of embryos shown in F,H and J, respectively (approximate position of sections are indicated by bars in F,H,J). (G′,I′,K′) Higher magnifications of G,I,K, respectively. ADE, anterior definitive endoderm; AVE, anterior visceral endoderm; al, allantois; de, definitive endoderm; ec, ectoderm; ep, epiblast (thickness indicated by a bar); m, mesoderm; pp, prechordal plate; ps, primitive streak (indicated by dotted lines in F,H); ve, visceral endoderm (thickness indicated by arrowheads). Dashed lines in G′,I′,K′ indicate positions of AVE, ADE and pp, respectively. (M) In situ hybridization of *Ssdp1* on a section of E9.0 embryo. The hybridization signals appeared brown. (N) Whole-mount in situ hybridization showing the reduced expression of *Ssdp1* in *hsk* homozygous embryos. Embryos were grouped according to their genotypes, and were subjected to whole-mount in situ hybridization, performed at the same time in different wells. Similar results were obtained by two independent experiments. Scale bars: 200 μm in L,N; 100 μm in F,H,I,J,K,M; 20 μm in G,G′,I′,K′. (O) Northern blot analysis of E9.5 RNA showing expression of *Ssdp1* RNA in *hsk* homozygous embryos at a reduced level. (P) Relative expression levels of the genes surrounding the transgene insertion site in *hsk* mutants compared with wild type. Values shown represent the means and standard errors of the relative expression levels. The number on each bar indicates the number of samples analyzed. The expression level of *Ssdp1* in *hsk* heterozygotes (**P*<0.01) and homozygotes (***P*<0.001) was reduced.

site in the C5-C6 region of chromosome (Chr) 4 (Fig. 2A-D). Cloning the genomic DNA fragments flanking the transgene insertion site localized the affected region to a 105.85 Mb segment of Chr 4, consistent with the chromosomal FISH results. Further analysis showed that four copies of the transgene were inserted into intron 4 of the *Ssdp1* locus, accompanying a 9 bp deletion (Fig. 2E).

As *Ssdp1* appeared to be a good candidate for the gene disrupted in *hsk* mutants, we analyzed the expression pattern of *Ssdp1* in wild-type embryos. *Ssdp1* was widely expressed in wild-type embryos from E6.5 to E9.0 (Fig. 2F-M). At E6.5, *Ssdp1* mRNA was localized to the basal margin of epiblast cells but was absent from the visceral endoderm, including the early head organizer tissue, the AVE (Fig. 2G,G′). However, *Ssdp1* expression was detected in the later head organizer tissues, including the ADE (Fig. 2I,I′), prechordal plate and foregut epithelium (Fig. 2K,K′). By E9.0, *Ssdp1* was ubiquitously expressed (Fig. 2M). Whole-mount in situ hybridization of mutant embryos at late head fold (LHF) stage to E8.0 revealed that the expression of *Ssdp1* in *hsk* homozygotes was clearly reduced compared with wild type, although the pattern of expression was unaltered (Fig. 2N). Northern blot analysis of RNA extracted from E9.5 embryos detected two *Ssdp1*-positive bands at 2.3 kb and 3.8 kb (Fig. 2O), similar to results observed using rat *Ssdp1* RNA (Raval-Fernandes et al., 1999). The *Ssdp1* RNA species detected in *hsk* homozygotes were of normal size, but their expression levels were reduced to ~32% of the level seen in wild-type embryos (Fig. 2O,P). No significant differences were detected in the expression levels of the genes surrounding *Ssdp1* (Fig. 2E,P). Thus, the transgene insertion results in the specific downregulation of *Ssdp1* expression.

To test whether the loss of anterior head structures was caused by reduced expression of *Ssdp1*, we designed a transgene in which *Ssdp1* is under the control of a ubiquitous promoter (Fig. 3A) and established two transgenic mouse lines (TG). These transgenic mice were crossed with *Ssdp1*$^{+/hsk}$ mutants, and the resultant progeny (TG/*Ssdp1*$^{+/hsk}$) were crossed with *Ssdp1*$^{+/hsk}$ mice. In one transgenic line, number 37, TG37/*Ssdp1*$^{hsk/hsk}$ embryos did not show any of the head defects or growth retardation observed in *Ssdp1*$^{hsk/hsk}$ mutants at E9.5 (Fig. 3B,C), and TG37/*Ssdp1*$^{hsk/hsk}$ mice developed into healthy and fertile adults (Fig. 3E). In the other line, number 141, which expressed the *Ssdp1* at a lower level than number 37 (Fig. 3F), only partial rescue was observed at E9.5 (Fig. 3D), and no live-born TG141/*Ssdp1*$^{hsk/hsk}$ mice were obtained. Together with the mapping and expression data, these results suggest that the *hsk* mutant phenotype results from reduced expression of *Ssdp1*.

Development of the prechordal plate is compromised in *Ssdp1* mutants

The severe defects in anterior head development of *Ssdp1* mutants suggest that this phenotype is associated with defects in the head induction process. To test this possibility, we examined the development of the head organizer in *Ssdp1* mutants. Proper head development first requires the anterior patterning activity of the AVE, which expresses *Lefty1*, *Lim1*, *Cerl*, and *Hhex* (Fig. 4A,C; data not shown) at early streak (ES, E6.5) and mid-streak (MS, E6.75) stages. Subsequently, the AVE is displaced by the ADE, which is derived from the anterior primitive streak and is marked by the expression of *Hhex* and *Cerl* at early bud (EB) stage (E7.25) (Fig. 4E,G). Expression of these genes was unaltered in *Ssdp1* mutants (Fig. 4B,D,F,H; data not shown), suggesting that the AVE and ADE developed normally.

Slightly later, at early head fold (EHF) stage (E7.5), another head organizer tissue, prechordal plate, begins to form at the anterior portion of the axial mesoendoderm. *Cerl* is expressed

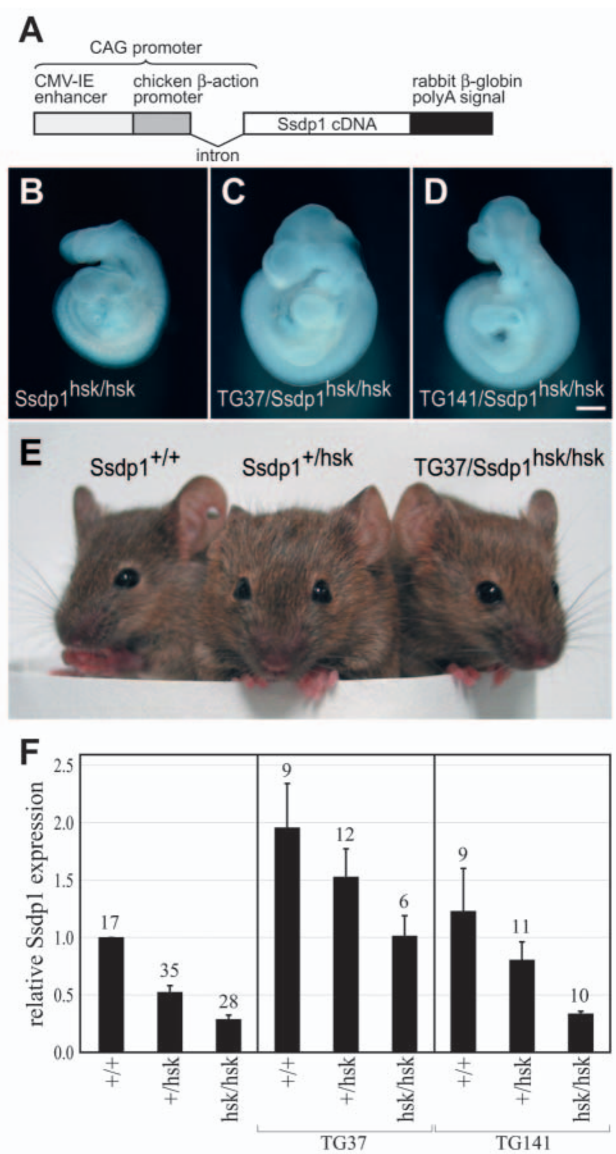

Fig. 3. Rescue of the *Ssdp1*$^{hsk/hsk}$ mutant phenotype by the *Ssdp1* transgene. (A) Structure of the *Ssdp1* transgene (TG). (B-D) Lateral view of E9.5 embryos obtained by the cross of TG#37/*Ssdp1*$^{+/hsk}$ or TG#141/*Ssdp1*$^{+/hsk}$ with *Ssdp1*$^{+/hsk}$ mice. (B) *Ssdp1*$^{hsk/hsk}$ embryo. (C) Completely rescued *Ssdp1*$^{hsk/hsk}$ embryo carrying TG#37. (D) Partially rescued *Ssdp1*$^{hsk/hsk}$ embryo carrying TG#141. Scale bar: 400 μm for B-D. (E) TG#37 completely rescues the mutant phenotype. (F) The expression level of *Ssdp1* in two TG lines. Values shown represent the means and standard errors of the relative expression levels of the sum of endogenous and transgenic *Ssdp1* RNA, as quantified by RT-PCR. The number on each bar indicates the number of samples analyzed.

in the prechordal plate (Fig. 4I, arrow), as well as the anterior mesoderm and anterior definitive endoderm. In *Ssdp1* mutants, *Cerl* expression in the prechordal plate was either strongly reduced or absent (Fig. 4J, arrow), while expression in other tissues was not significantly altered. Similarly, *Dkk1,* which is normally expressed in the anterior-most domain of the prechordal plate and in the anterior margin of the head mesoderm, was specifically absent from the prechordal plate of late head fold (LHF) stage mutants (E7.75, Fig. 4K,L, arrow). *Foxa2* and *Gsc*, which are normally expressed in the prechordal plate in E8.0 (1-2 somites) embryos (Fig. 4M,O, arrow), were also absent from the anterior midline of *Ssdp1* mutants, suggesting an abnormal development of the prechordal plate (Fig. 4N,P). The prechordal plate can be morphologically distinguished at E8.0 from its surrounding tissues by two characteristics: (1) it directly contacts the neuroectoderm, and (2) it is thicker than the neighboring notochordal plate (Fig. 4Q,S, arrowheads). In *Ssdp1* mutants, the tissue anterior to the notochordal plate either failed to contact the neuroectoderm or had a similar thickness as the notochordal plate, or both (Fig. 4R,T, anterior end of notochordal plate is indicated by an arrowhead; data not shown), indicating the lack of a differentiated prechordal plate. In summary, the development of the AVE and ADE is normal until EB stage in *Ssdp1* mutants, but the development of the prechordal plate is compromised from EHF stage onwards.

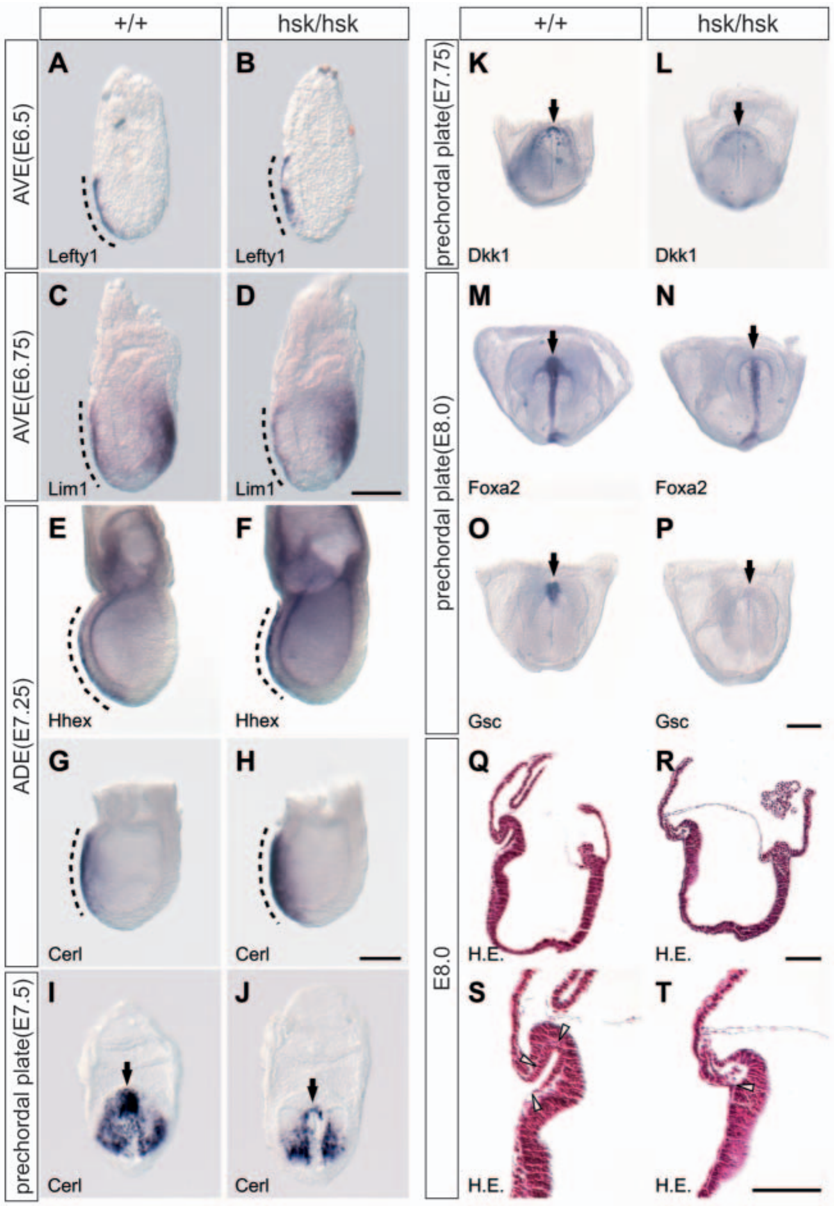

Fig. 4. Expression of anterior patterning markers in $Ssdp1^{hsk/hsk}$ mutants. In situ hybridization showing gene expression in the anterior visceral endoderm (AVE) (A-D), anterior definitive endoderm (ADE) (E-H) and the prechordal plate (I-P) in wild-type and $Ssdp1^{hsk/hsk}$ mutants. Wild-type (A) and mutant (B, *n*=5/5) expression of *Lefty1*; wild-type (C) and mutant (D, *n*=7/7) expression of *Lim1*; wild-type (E) and mutant (F, *n*=4/4) expression of *Hhex*; wild-type (G,I) and mutant (H, *n*=4/4; J, *n*=2/9) expression of *Cerl*; wild-type (K) and mutant (L, *n*=0/6) expression of *Dkk1*, wild type (M) and mutant (N, *n*=0/6) expression of *Foxa2*, and wild-type (O) and mutant (P, *n*=0/3) expression of *Gsc*. *n*, number of embryos expressing the gene/number of embryos analyzed. Broken lines in A-D and E-H indicate the AVE and ADE, respectively. Arrows in I-P indicate the prechordal plate. (Q-T) Sagittal section of wild-type (Q,S) and mutant (R,T) embryos stained with Hematoxylin and Eosin. Scale bars: in D, 100 µm for A-D; in H, 100 µm for E-H; in P, 200 µm for I-P; in R, 200 µm for Q,R; in T, 200 µm for S,T.

Ssdp1 mutants fail to maintain head structures anterior to the midbrain-hindbrain boundary

To understand how this late onset head organizer defect in *Ssdp1* mutants affects head development, we examined the extent of regionalization of anterior neuroectoderm. From EHF to LHF stage, the anteriormost neuroectoderm of wild-type embryos is marked by *Six3* and *Foxd4* (*Fkh2*) expression (Fig. 5A; data not shown). Approximately half of the *Ssdp1* mutants expressed these genes, although expression was generally reduced in strength and in extent (Fig. 5B; data not shown). *Otx2* expression, which marks the prospective forebrain and midbrain regions (Fig. 5C), was detected in all *Ssdp1* mutants at E8.0, although the size of the expression domain was slightly reduced (Fig. 5D). These results suggest that anterior head development is initiated in *Ssdp1* mutants between EHF stage and E8.0, although the most anterior neuroectoderm fates may not be specified in some embryos.

At E8.5 (8-10 somites), *Six3* and *Otx2* are expressed at the anterior margin of the neural plate, with *Six3* marking the forebrain and *Otx2* extending more caudally to mark the midbrain (Fig. 5E,G). In *Ssdp1* mutants, *Six3* was not expressed (Fig. 5F), while expression of *Otx2* was either absent or confined to the anterior-most tip of the embryo (Fig. 5H; data not shown). Furthermore, *Foxg1* (*BF1*) and *Pax6*, which normally mark the telencephalon and the diencephalon, respectively, were not expressed in *Ssdp1* mutants (Fig. 5I,J; data not shown). The midbrain-hindbrain boundary (MHB) markers *En2*, *Fgf8* and *Wnt1* were either absent from the region corresponding to the MHB or expressed at the anterior tip in *Ssdp1* mutants (Fig. 5K-P; data not shown). Expression of *Krox20* in rhombomeres 3 and 5 of the hindbrain and of *Uncx4.1* in the somites was unaltered in *Ssdp1* mutants at E8.5-9.5 (Fig. 5M,N; data not shown). These results suggest that the head neuroectoderm anterior to the MHB was initially specified, but was lost by E8.5 in some *Ssdp1* mutants, while the posteriormost region of the midbrain was maintained in others.

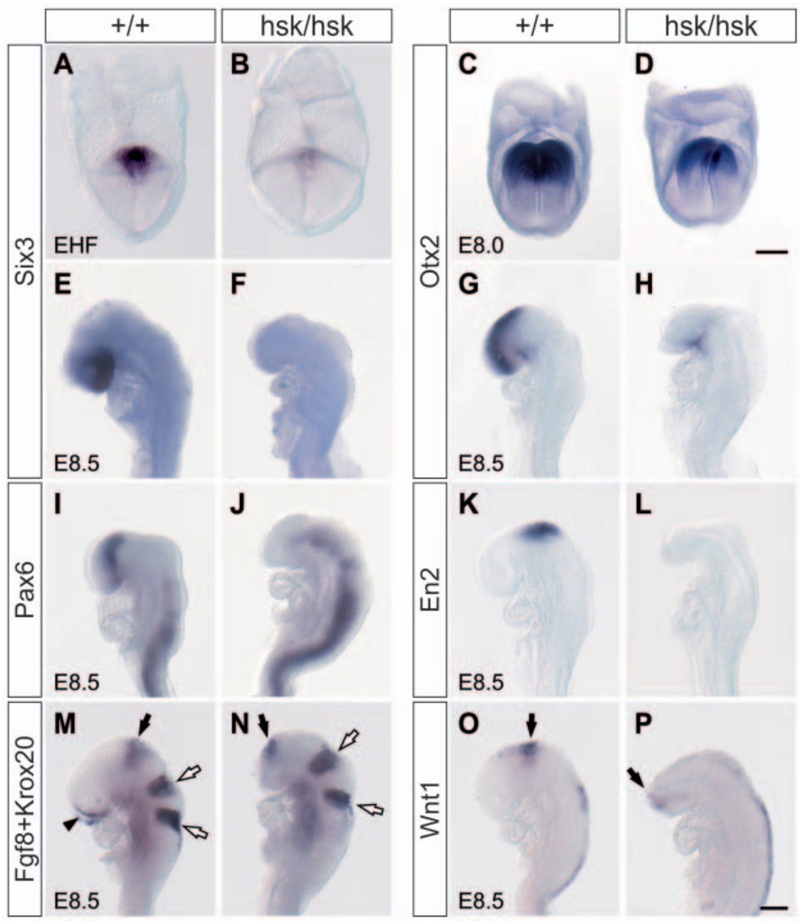

Fig. 5. Head defects in *Ssdp1*$^{hsk/hsk}$ mutants. In situ hybridization showing the expression of various regional markers in wild-type and *Ssdp1*$^{hsk/hsk}$ embryos. Wild-type (A,E) and mutant *Six3* expression (B, *n*=2/5; F, *n*=0/8); wild-type (C,G) and mutant (D, *n*=7/7; H, *n*=1/5) *Otx2* expression; wild-type (I) and mutant (J, *n*=0/2) *Pax6* expression; and wild-type (K) and mutant (L, *n*=2/3) *En2* expression. (M,N) *Fgf8* was expressed in the commissural plate (arrowhead) and MHB (black arrow) in wild-type embryos (M), while MHB expression in *Ssdp1*$^{hsk/hsk}$ mutants was observed at the anterior tip (black arrow in N, *n*=6/10). Expression of *Krox20* was unaffected (M,N, white arrows). (O,P) *Wnt1* expression in the MHB (O; arrow) was observed at the anterior tip in some *Ssdp1*$^{hsk/hsk}$ mutants (arrow in P, *n*=3/5). Scale bars: in D, 200 µm for A-D; in P, 400 µm for E-P.

Changes in apoptosis and cell proliferation do not cause the initial loss of anterior neuroectoderm in *Ssdp1* mutants

To determine whether the absence of the anterior neuroectoderm of E8.5 *Ssdp1* mutants is caused by the loss or reduced growth of previously specified anterior neuroectoderm, we examined apoptosis and cell proliferation using TUNEL and anti-PCNA antibody staining in these embryos. At E8.0 and E8.5, no significant difference in apoptosis was observed between wild-type and *Ssdp1* homozygous embryos (Fig. 6A-D). At E9.0 (16-18 somites), however, there was a significant increase in the number of apoptotic cells in the degenerating head neuroectoderm and somites of mutant embryos (data not shown). At E8.0, the level of cell proliferation was similar between wild-type and *Ssdp1* mutant embryos (Fig. 6G). However, at E8.5 and E9.0, the global increase in cell proliferation observed in wild-type embryos (Fig. 6H; data not shown) was greatly attenuated in all tissues examined in *Ssdp1* mutants (Fig. 6E,F,H; data not shown). These results suggest that changes in apoptosis and cell proliferation do not account for the specific loss of anterior neuroectoderm in E8.5 *Ssdp1* mutants. The strong, global reduction of cell proliferation and increase in apoptosis in E9.0 somites may, however, contribute to the widespread growth retardation of *Ssdp1* mutants (Fig. 1Q).

Ssdp1 is an activator component of the Ssdp1-Lim1-Ldb1 complex

Ssdp1 has been shown to interact biochemically with Ldb1 (Chen et al., 2002; van Meyel et al., 2003), a co-factor of LIM domain proteins such as Lim1 (Agulnick et al., 1996). As *Ssdp1* mutant embryos have defects in head organizer development, which requires *Lim1* activity, we hypothesized that Ssdp1 forms a complex with Lim1 through Ldb1 binding and regulates the transcriptional activity of this complex in the late head organizer. Indeed, co-expression of *Ssdp1*, *Lim1* and *Ldb1* in the prechordal plate, as revealed by in situ hybridization of *Ssdp1* and *Ldb1* and β-galactosidase staining of *Lim1-lacZ* knock-in embryos, hints at the presence of the Ssdp1-Lim1-Ldb1 ternary complex in this tissue and/or its precursor (Fig. 2K, Fig. 7A-D; data not shown).

To reveal the molecular function of Ssdp1, we first analyzed the transcriptional activity of Ssdp1 using a GAL4-UAS system in P19 embryonic carcinoma cells. The effector, a fusion protein of the DNA-binding domain of GAL4 and full-length Ssdp1, activated reporter gene expression via GAL4-binding sites in a dose-dependent manner in transfected cells (Fig. 7E,F). Thus, Ssdp1 contains a transcriptional activation domain.

To study the role of Ssdp1 in the regulation of Lim1-Ldb1-dependent transactivation, we used the *Xenopus Gsc* promoter (up to –492 bp) to drive expression of a reporter gene (Fig. 7G). This promoter has previously been shown to be regulated by a Lim1-Ldb1 complex through two elements, UE and DE (Mochizuki et al., 2000). As *Gsc* expression was lost in *Ssdp1* mutants (Fig. 4P), it seemed a likely target for a complex including Lim1, Ldb1 and Ssdp1. Neither Ldb1 nor Ssdp1

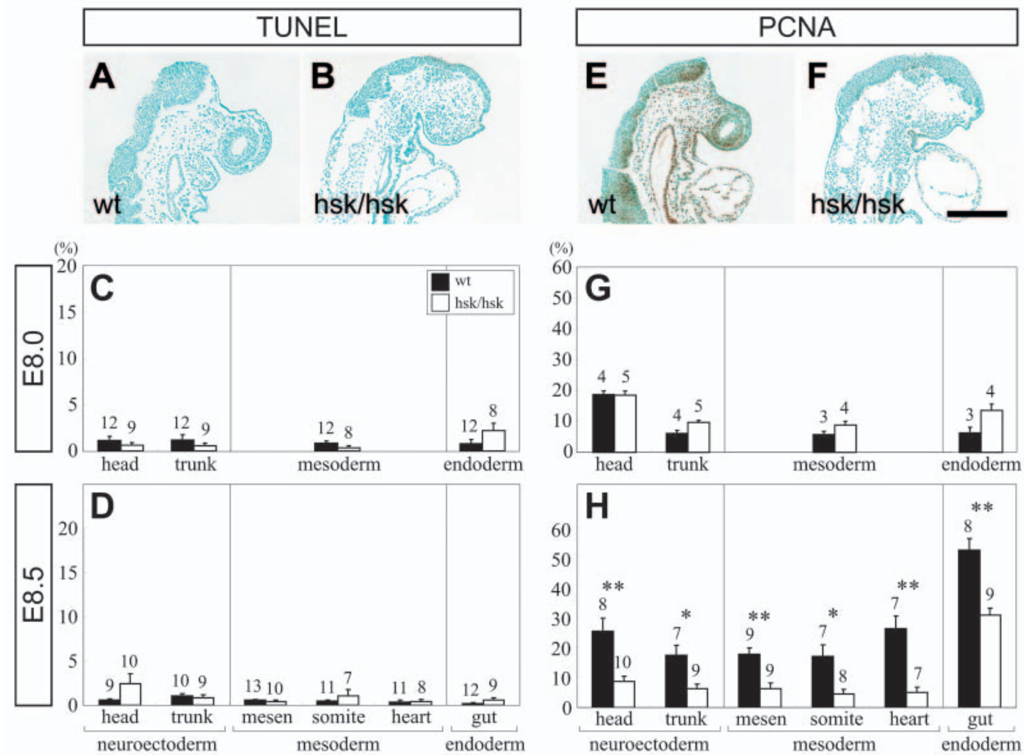

Fig. 6. Apoptosis and cell proliferation in *Ssdp1*$^{hsk/hsk}$ mutants. Sections showing the distribution of apoptotic (A,B) and proliferating (E,F) cells in the head region of wild-type (A,E) and *Ssdp1*$^{hsk/hsk}$ mutant (B,F) embryos. (D) Scale bar in F, 400 μm for A,B,E,F. (C,D,G,H) Quantitation of apoptotic and proliferating cells in various tissues of wild type and *Ssdp1*$^{hsk/hsk}$ mutants at E8.0 and E8.5. Values shown represent the means and standard errors of the percentages of the apoptotic (C,D) or proliferating (G,H) cells to total cells. Black and white bars represent wild-type and *Ssdp1*$^{hsk/hsk}$ mutant embryos, respectively. The number above each bar indicates the number of samples analyzed. The tissues with significant differences between wild-type and mutant are indicated (*P<0.05, **P<0.01). mesen, mesenchyme.

alone was able to activate the *Gsc* promoter in transfected cells, while Lim1 was able to activate the promoter by itself, probably through interactions with endogenous Ldb1 and Ssdp1. Co-expression of Ldb1 or Ssdp1 with Lim1 slightly enhanced the activation, while co-expression of all three proteins strongly increased expression of the reporter gene (Fig. 7H). Moreover, Ssdp1 enhanced transactivation in a dose-dependent manner in the presence of Ldb1 (Fig. 7I). These results suggest that Ssdp1 enhances the activator function of the Lim1-Ldb1 complex. This supports our hypothesis that Ssdp1 functions by forming a ternary complex with Lim1 and Ldb1, and acting as an activator component of the complex (Fig. 7J). Therefore, it is likely that the reduced expression of *Ssdp1* in *hsk* homozygous embryos decreases the transcriptional activity of the Lim1 complex in the prechordal plate, resulting in its abnormal development.

Ssdp1 interacts genetically with *Lim1* and *Ldb1* in head development and body growth

If Ssdp1 functions by forming a Lim1-Ldb1-Ssdp1 ternary complex during development, the simultaneous reduction of Ssdp1 and either Lim1 or Ldb1 should reduce the amount of this complex and cause similar developmental defects as observed in *Ssdp1* mutants. We tested this hypothesis by making compound heterozygous mutant embryos. All of the *Ssdp1*$^{+/hsk}$ (n=6) and *Lim1*$^{+/–}$ (n=10) embryos obtained by crossing *Ssdp1*$^{+/hsk,}$ and *Lim1*$^{+/–}$ mice appeared normal at E9.0-9.5 (data not shown), whereas *Ssdp1*$^{+/hsk}$*;Lim1*$^{+/–}$ embryos exhibited variable phenotypes that could be classified into three categories. Type I embryos showed no obvious defects (Fig. 8B). Type II embryos exhibited microcephaly with relatively normal body size (Fig. 8C), while type III embryos showed severe growth retardation in addition to microcephaly, and failed to undergo embryonic turning (Fig. 8D).

The majority of *Ssdp1*$^{+/hsk}$ (normal/total=6/7) and *Ldb1*$^{+/–}$ (n=6/7) mutants obtained from crosses between *Ssdp1*$^{+/hsk}$ and *Ldb1*$^{+/–}$ mice appeared normal at E9.0-9.5 (Fig. 8E). Other single mutants displayed mild growth retardation and mild microcephaly (data not shown). Phenotypic differences between *Ssdp1*$^{+/hsk}$ embryos obtained from different crosses may reflect differences in genetic background between *Lim1* (ICR) and *Ldb1* (C57BL/6) mutants. Approximately half of the *Ssdp1*$^{+/hsk}$;*Ldb1*$^{+/–}$ embryos appeared normal (Fig. 8F), while the remaining mutants showed varying degrees of microcephaly and growth retardation that were difficult to classify (Fig. 8G). The incomplete penetrance of *Ssdp1*$^{+/hsk}$*; Lim1*$^{+/–}$ and *Ssdp1*$^{+/hsk}$; *Ldb1*$^{+/–}$ phenotypes may reflect the fact that *hsk* is not a null mutation. However, these results indicate that *Ssdp1* genetically interacts with *Lim1* and *Ldb1* in both head development and body growth, which is consistent with the model that the Ssdp1-Lim1-Ldb1 complex regulates these developmental processes in vivo.

Discussion

Ssdp1 regulates head development as an activator component of a Ssdp1-Lim1-Ldb1 complex

Head development is initiated by the AVE and maintained by the anterior AME, which is comprised of the ADE and the prechordal plate. The development of all of these head organizer tissues requires the function of *Lim1* (Shawlot and Behringer, 1995; Shawlot et al., 1999). Both *Lim1* and *Ldb1* mutant embryos have a constriction at the embryonic/extra-embryonic boundary at E7.5 and lack head structures anterior to rhombomere 3 at E8.5 (Mukhopadhyay et al., 2003; Shawlot

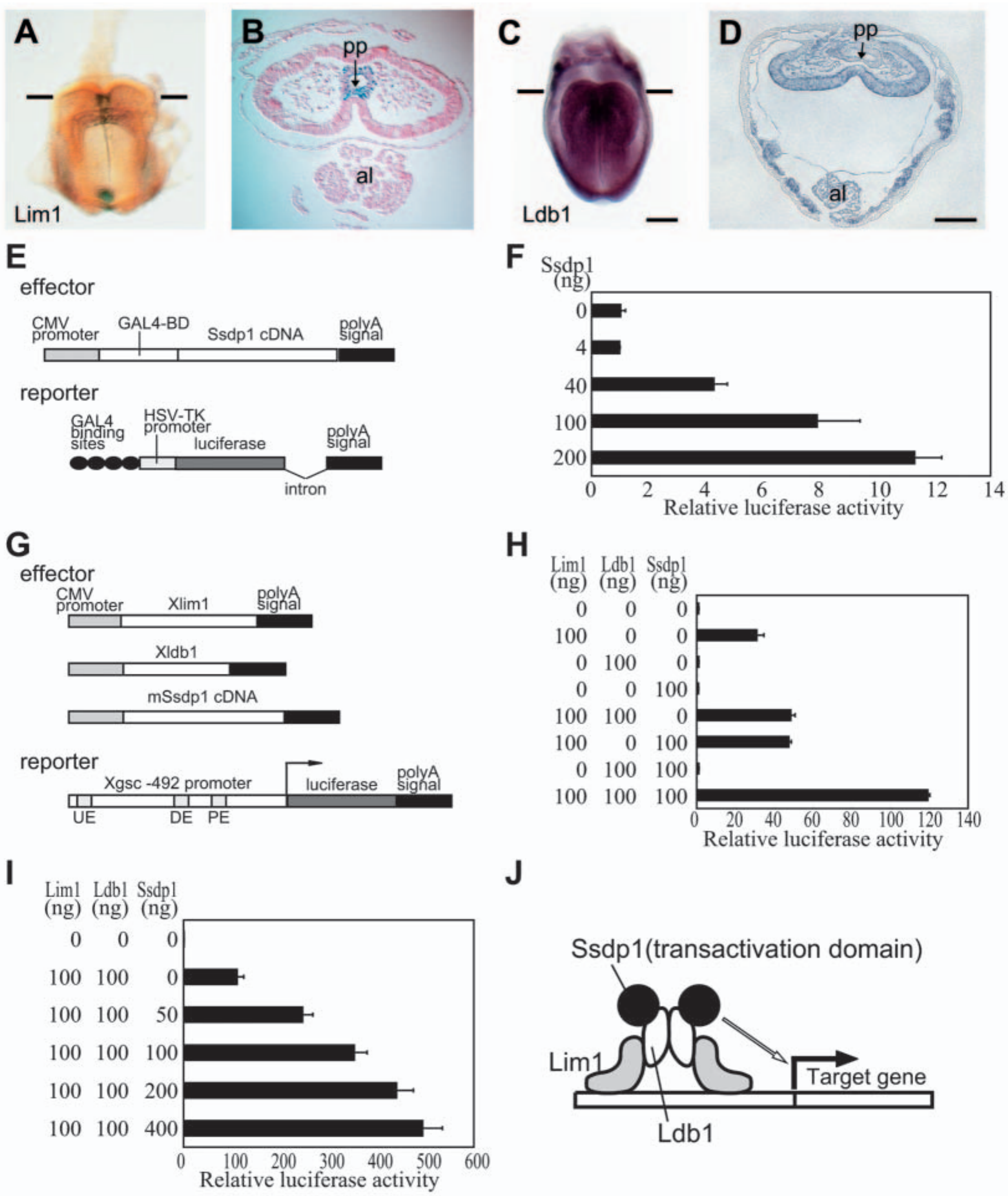

Fig. 7. Ssdp1 acts as a co-activator component of a Lim1-Ldb1-Ssdp1 complex. (A) E8.0 *Lim1-lacZ* knock-in embryo stained for β-galactosidase activity. (B) Cross-section of the embryo shown in A; approximate sectioning position is indicated in A. (C) Whole-mount in situ hybridization of Ldb1 in E8.0 embryo. (D) Cross-section of embryo shown in C. Scale bars in C,D: 200 μm. (E) Schematic representation of the effector and the reporter plasmid used in the transfection assay described in F. (F) The fusion protein comprised of the GAL4 DNA-binding domain and Ssdp1 activated reporter gene expression in a dose-dependent manner. (G) Schematic representation of the effectors and a reporter used in the transfection assays described in H and I. (H) Effects of Lim1, Ldb1 and Ssdp1 on the *Gsc* promoter. (I) Effects of varying Ssdp1 concentration on the activity of Lim1- and Ldb1-mediated reporter gene expression. Values are the means and standard errors of duplicate experiments. (J) A model for the action of Ssdp1. Ssdp1, Ldb1 and Lim1 constitute a ternary complex and regulate genes expressed in the prechordal plate.

and Behringer, 1995), suggesting that Lim1 and Ldb1 make a functional complex in vivo that is crucial for development of gastrulation stage mouse embryos.

Experimental removal or transplantation of anterior AME at EHF stage has demonstrated the crucial role of the prechordal plate in anterior head development (Camus et al., 2000). Our analysis of *hsk* mutant embryos demonstrates the essential role of *Ssdp1* in prechordal plate development after the EHF stage. The head defects observed in *Ssdp1* mutants resembled those of chimeric embryos lacking *Lim1* in all embryonic tissues, including the prechordal plate, suggesting a strong link between Ssdp1 and Lim1 in prechordal plate development (Shawlot et al., 1999). Co-expression of *Ssdp1*, *Lim1* and *Ldb1* in the prechordal plate as well as genetic interactions between *Ssdp1* and *Lim1* or *Ldb1* in head development strongly supports the hypothesis that these three proteins constitute a functional complex in vivo. In addition to the co-activator function of Ssdp1 in transfected cells, downregulation of the Lim1 target genes *gsc* (Mochizuki et al., 2000) and *Foxa2* (Shawlot and Behringer, 1995) in *Ssdp1* mutants suggests a model in which Ssdp1 is an essential activator component of the Ssdp1-Lim1-Ldb1 complex in the prechordal plate. As each Ssdp molecule has been suggested to bind to a single Ldb1 molecule (van Meyel et al., 2003), the functional complex should consist of $(Ssdp1)_2$-$(Lim1)_2$-$(Ldb1)_2$ (Fig. 7J).

The head defects of *Ssdp1* mutants also resemble those of chimeric embryos lacking *Otx2* function in the embryonic tissues, including the anterior AME (Rhinn et al., 1998), or of mutants lacking *Otx2* function specifically in the neuroectoderm (Kurokawa et al., 2004; Suda et al., 1999), raising the possibility that reduced Otx2 activity in the anterior AME and/or neuroectoderm also contributes to the headless phenotype of *Ssdp1* mutants. As Lim1 and Otx2 proteins have been shown to interact biochemically (Nakano et al., 2000), it

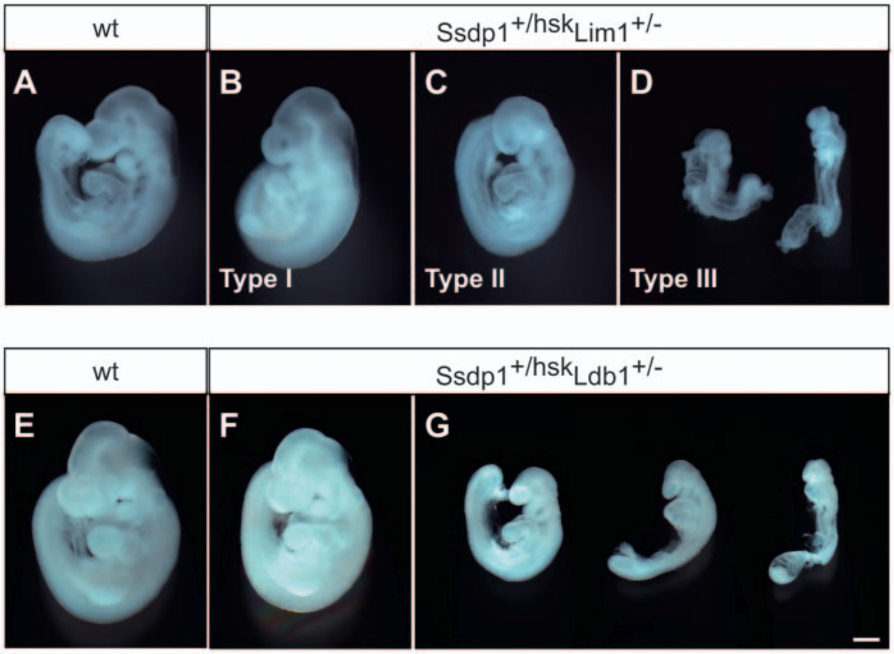

Fig. 8 Genetic interactions of *Ssdp1* with *Lim1* and *Ldb1*. (A-D) E9.5 embryos obtained by crossing $Ssdp1^{+/hsk}$ and $Lim1^{+/-}$ mice. (A) Wild-type embryo. (B-D) Double heterozygotes, which can be classified into three types: I, normal (B, *n*=6); II, microcephaly (C, *n*=5); III, dwarfism (D, *n*=4). (E-G) E9.5 embryos obtained by crossing $Ssdp1^{+/hsk}$ and $Ldb1^{+/-}$ mice. (E) Wild-type embryo. (F,G) Double heterozygotes showing no apparent abnormalities (F, *n*=7) or varying degrees of abnormality (G, *n*=6). Scale bar: 400 μm.

is possible that Ssdp1 also functions by forming a complex that includes Ldb1, Lim1 and Otx2. However, although interaction of Ldb1 with the Otx-type homeodomain protein Pitx1 (Bach et al., 1997) suggests that Otx2 function might be regulated by Ssdp1 independently of Lim1, the sequence similarities between Otx2 and Pitx1 are limited to the homeodomain, which is itself insufficient for interaction with Ldb1. To date, there is no direct evidence for an interaction between Otx2 and Ldb1, but this possibility should be addressed in the future.

Role of the prechordal plate in head development

Studies in lower vertebrates have suggested that the role of the prechordal plate in head development is to protect the overlying anterior neuroectoderm from posteriorizing Wnt signals and ventralizing BMP signals (Glinka et al., 1997). A similar role for the prechordal plate in the mouse was also suggested by the absence of anterior head structures in mice that lack the Wnt antagonist Dickkopf1 and in double mutants lacking the two BMP antagonists Noggin and Chordin (Bachiller et al., 2000; Mukhopadhyay et al., 2001). However, the mechanism causing head defects in these embryos is not known.

In *Ssdp1* mutants, specification of anterior neuroectoderm was incomplete, suggesting that the prechordal plate at EHF stage is required for this process. Later loss of head neuroectoderm anterior to the MHB suggests that the prechordal plate is required for maintenance of the anterior neuroectoderm between E8.0 and E8.5. As changes in cell death and/or proliferation cannot account for the loss of anterior head tissues, the most likely reason for the loss of head structures is a change in gene expression patterns leading to the posterior transformation of neuroectoderm normally specified to become fore- or midbrain. This is consistent with the model that the prechordal plate after EHF stage promotes head development by maintaining the expression of anterior neuroectoderm genes by protecting this tissue from posteriorizing signals. Supporting this notion, expression of Dkk1, an antagonist of the posteriorizing signal Wnt, is lost in the prechordal plate of *Ssdp1* mutants. In addition, abnormal specification of the anterior neural plate may secondarily cause degeneration of anterior head tissue, as revealed by the increased apoptosis in E9.0 *Ssdp1* mutants. A similar increase in pyknotic cells in degenerating head tissue was also reported for two mutants lacking ADE and prechordal plate tissue (Vincent et al., 2003).

Ssdp1 regulates cell proliferation and body growth

Ssdp1 mutants exhibited a global reduction in cell proliferation after E8.5 and an increase in apoptosis in somites at E9.0. These changes may be at the root of the abnormalities such as growth retardation and kinked neural tube that were observed in *Ssdp1* mutants. Although the mechanism by which *Ssdp1* regulates cell proliferation is unknown at present, growth retardation of $Ssdp1^{+/hsk};Lim1^{+/-}$ and $Ssdp1^{+/hsk};Ldb1^{+/-}$ compound mutants suggests involvement of a Ssdp1-Lim1-Ldb1 complex in this process. A shortened body axis was also observed in embryos lacking either *Ldb1* or *Lim1*, supporting this hypothesis (Mukhopadhyay et al., 2003; Shawlot and Behringer, 1995). However, if the Lim1 complex plays a major role in the regulation of cell proliferation and cell death, it must be through an indirect mechanism, as *Lim1* is not expressed in all of the affected cells. It is conceivable that defective gastrulation movements (Hukriede et al., 2003; Tam et al., 2004) or the inability of cells with reduced Lim1 complex activity to induce lateral plate mesoderm genes (Tsang et al., 2000) secondarily affects the proliferation and survival of surrounding cells. Furthermore, it is possible that Ssdp1 may also function independently of Lim1, in which case the Ldb1-Ssdp1 complex may regulate cell proliferation in a cell-autonomous manner by controlling the activities of transcription factors involved in cell cycle regulation and cell survival. Alternatively, Ssdp1 might play a direct role in the DNA replication process as a single stranded DNA-binding protein (Bayarsaihan et al., 1998).

Conclusion

Analysis of *hsk* mutants showed that disruption of the *Ssdp1* gene and the resulting reduction in *Ssdp1* expression causes defects in the prechordal plate development and anterior truncations, with some mutants also exhibiting smaller body size. In vitro data demonstrated that Ssdp1 acts as a co-activator that enhances transcriptional activation by the Lim1-

Ldb1 complex. Moreover, genetic interactions between *Ssdp1* and *Lim1* or *Ldb1* suggest that the phenotypes observed in *Ssdp1* mutants very probably reflect reduced activity of a Lim1 complex. Together, our data demonstrate that Ssdp1 acts as an essential activator component of a Ssdp1-Lim1-Ldb1 complex in the development of the prechordal plate and body growth.

We thank Ms Y. Minami for excellent technical assistance; Dr S. Aizawa and LARGE members for mouse embryo manipulations and the housing of mice; Drs I. Matsuo and C. Kimura-Yoshida for technical advice; Dr P. Tam for help on staging and histology of embryos; Drs A. Sawada and S. Yamamoto for helpful discussions; Drs A. Shimono, E. Lai, E. DeRobertis, C. Niehrs, A. Joyner, G. Martin, B. Hogan, K. Kaestner, P. Thomas, D. Wilkinson, H. Hamada, S.-L. Ang, A. Mansouri, P. Gruss, A. McMahon, I. Matsuo, J.-I. Miyazaki, H. Niwa, M. Taira, K. W. Cho and M. Hibi for reagents. N.N. is a recipient of a fellowship from the Japan Society for the Promotion of Science (JSPS). This work was supported by grants from the Ministry of Education, Science, Culture, Sports, Science, and Technology of Japan (MEXT) (14034230), JSPS (14380345) and RIKEN to H.S., and a grant from MEXT to H.K. (12CE2007).

References

Agulnick, A. D., Taira, M., Breen, J. J., Tanaka, T., Dawid, I. B. and Westphal, H. (1996). Interactions of the LIM-domain-binding factor Ldb1 with LIM homeodomain proteins. *Nature* **384**, 270-272.

Ang, S. L., Conlon, R. A., Jin, O. and Rossant, J. (1994). Positive and negative signals from mesoderm regulate the expression of mouse *Otx2* in ectoderm explants. *Development* **120**, 2979-2989.

Bach, I. (2000). The LIM domain: regulation by association. *Mech. Dev.* **91**, 5-17.

Bach, I., Carriere, C., Ostendorff, H. P., Andersen, B. and Rosenfeld, M. G. (1997). A family of LIM domain-associated cofactors confer transcriptional synergism between LIM and Otx homeodomain proteins. *Genes Dev.* **11**, 1370-1380.

Bachiller, D., Klingensmith, J., Kemp, C., Belo, J. A., Anderson, R. M., May, S. R., McMahon, J. A., McMahon, A. P., Harland, R. M., Rossant, J. et al. (2000). The organizer factors Chordin and Noggin are required for mouse forebrain development. *Nature* **403**, 658-661.

Bachy, I., Failli, V. and Retaux, S. (2002). A LIM-homeodomain code for development and evolution of forebrain connectivity. *NeuroReport* **13**, A23-A27.

Barnes, J. D., Crosby, J. L., Jones, C. M., Wright, C. V. and Hogan, B. L. (1994). Embryonic expression of *Lim-1,* the mouse homolog of *Xenopus Xlim-1*, suggests a role in lateral mesoderm differentiation and neurogenesis. *Dev. Biol.* **161**, 168-178.

Bayarsaihan, D., Soto, R. J. and Lukens, L. N. (1998). Cloning and characterization of a novel sequence-specific single-stranded-DNA-binding protein. *Biochem. J.* **331**, 447-452.

Beddington, R. S. and Robertson, E. J. (1999). Axis development and early asymmetry in mammals. *Cell* **96**, 195-209.

Belo, J. A., Bouwmeester, T., Leyns, L., Kertesz, N., Gallo, M., Follettie, M. and de Robertis, E. M. (1997). Cerberus-like is a secreted factor with neutralizing activity expressed in the anterior primitive endoderm of the mouse gastrula. *Mech. Dev.* **68**, 45-57.

Blum, M., Gaunt, S. J., Cho, K. W., Steinbeisser, H., Blumberg, B., Bittner, D. and de Robertis, E. M. (1992). Gastrulation in the mouse: the role of the homeobox gene *goosecoid*. *Cell* **69**, 1097-1106.

Camus, A., Davidson, B. P., Billiards, S., Khoo, P., Rivera-Perez, J. A., Wakamiya, M., Behringer, R. R. and Tam, P. P. (2000). The morphogenetic role of midline mesendoderm and ectoderm in the development of the forebrain and the midbrain of the mouse embryo. *Development* **127**, 1799-1813.

Chen, L., Segal, D., Hukriede, N. A., Podtelejnikov, A. V., Bayarsaihan, D., Kennison, J. A., Ogryzko, V. V., Dawid, I. B. and Westphal, H. (2002). Ssdp proteins interact with the LIM-domain-binding protein Ldb1 to regulate development. *Proc. Natl. Acad. Sci. USA* **99**, 14320-14325.

Crossley, P. H. and Martin, G. R. (1995). The mouse *Fgf8* gene encodes a family of polypeptides and is expressed in regions that direct outgrowth and patterning in the developing embryo. *Development* **121**, 439-451.

Downs, K. M. and Davies, T. (1993). Staging of gastrulating mouse embryos by morphological landmarks in the dissecting microscope. *Development* **118**, 1255-1266.

Glinka, A., Wu, W., Onichtchouk, D., Blumenstock, C. and Niehrs, C. (1997). Head induction by simultaneous repression of Bmp and Wnt signalling in *Xenopus*. *Nature* **389**, 517-519.

Glinka, A., Wu, W., Delius, H., Monaghan, A. P., Blumenstock, C. and Niehrs, C. (1998). Dickkopf-1 is a member of a new family of secreted proteins and functions in head induction. *Nature* **391**, 357-362.

Hatini, V., Tao, W. and Lai, E. (1994). Expression of winged helix genes, *BF-1* and *BF-2*, define adjacent domains within the developing forebrain and retina. *J. Neurobiol.* **25**, 1293-1309.

Henrique, D., Adam, J., Myat, A., Chitnis, A., Lewis, J. and Ish-Horowicz, D. (1995). Expression of a Delta homologue in prospective neurons in the chick. *Nature* **375**, 787-790.

Hiratani, I., Yamamoto, N., Mochizuki, T., Ohmori, S. Y. and Taira, M. (2003). Selective degradation of excess Ldb1 by Rnf12/RLIM confers proper Ldb1 expression levels and Xlim-1/Ldb1 stoichiometry in *Xenopus* organizer functions. *Development* **130**, 4161-4175.

Hobert, O. and Westphal, H. (2000). Functions of LIM-homeobox genes. *Trends Genet.* **16**, 75-83.

Hogan, B., Beddington, R., Constantini, F. and Lacy, E. (1994). Manipulating the Mouse Embryo: Laboratory Manual, 2nd edn. Cold Spring Harbor, New York: Cold Spring Harbor Laboratory Press.

Hukriede, N. A., Tsang, T. E., Habas, R., Khoo, P. L., Steiner, K., Weeks, D. L., Tam, P. P. and Dawid, I. B. (2003). Conserved requirement of Lim1 function for cell movements during gastrulation. *Dev. Cell* **4**, 83-94.

Joyner, A. L. and Martin, G. R. (1987). *En-1* and *En-2*, two mouse genes with sequence homology to the Drosophila engrailed gene: expression during embryogenesis. *Genes Dev.* **1**, 29-38.

Jurata, L. W., Kenny, D. A. and Gill, G. N. (1996). Nuclear LIM interactor, a rhombotin and LIM homeodomain interacting protein, is expressed early in neuronal development. *Proc. Natl. Acad. Sci. USA* **93**, 11693-11698.

Jurata, L. W., Pfaff, S. L. and Gill, G. N. (1998). The nuclear LIM domain interactor NLI mediates homo- and heterodimerization of LIM domain transcription factors. *J. Biol. Chem.* **273**, 3152-3157.

Kaestner, K. H., Monaghan, A. P., Kern, H., Ang, S. L., Weitz, S., Lichter, P. and Schutz, G. (1995). The mouse *fkh-2* gene. Implications for notochord, foregut, and midbrain regionalization. *J. Biol. Chem.* **270**, 30029-30035.

Kiso, M., Manabe, N., Komatsu, K., Nisioka, N., Nakai-Sugimoto, N. and Miyamoto, H. (2001). Abnormal accumulation of luteal bodies in ovaries of the senescence accelerated mouse (SAM). *J. Reprod. Dev.* **47**, 153-164.

Kurokawa, D., Takasaki, N., Kiyonari, H., Nakayama, R., Kimura-Yoshida, C., Matsuo, I. and Aizawa, S. (2004). Regulation of *Otx2* expression and its functions in mouse epiblast and anterior neuroectoderm. *Development* **131**, 3307-3317.

Mansouri, A., Yokota, Y., Wehr, R., Copeland, N. G., Jenkins, N. A. and Gruss, P. (1997). Paired-related murine homeobox gene expressed in the developing sclerotome, kidney, and nervous system. *Dev. Dyn.* **210**, 53-65.

Matsuda, Y. and Chapman, V. M. (1995). Application of fluorescence in situ hybridization in genome analysis of the mouse. *Electrophoresis* **16**, 261-272.

Meno, C., Ito, Y., Saijoh, Y., Matsuda, Y., Tashiro, K., Kuhara, S. and Hamada, H. (1997). Two closely-related left-right asymmetrically expressed genes, *lefty-1* and *lefty-2*: their distinct expression domains, chromosomal linkage and direct neuralizing activity in *Xenopus* embryos. *Genes Cells* **2**, 513-524.

Milan, M. and Cohen, S. M. (1999). Regulation of LIM homeodomain activity in vivo: a tetramer of dLDB and apterous confers activity and capacity for regulation by dLMO. *Mol. Cell* **4**, 267-273.

Mochizuki, T., Karavanov, A. A., Curtiss, P. E., Ault, K. T., Sugimoto, N., Watabe, T., Shiokawa, K., Jamrich, M., Cho, K. W., Dawid, I. B. et al. (2000). Xlim-1 and LIM domain binding protein 1 cooperate with various transcription factors in the regulation of the goosecoid promoter. *Dev. Biol.* **224**, 470-485.

Mukhopadhyay, M., Shtrom, S., Rodriguez-Esteban, C., Chen, L., Tsukui, T., Gomer, L., Dorward, D. W., Glinka, A., Grinberg, A., Huang, S. P. et al. (2001). Dickkopf1 is required for embryonic head induction and limb morphogenesis in the mouse. *Dev. Cell* **1**, 423-434.

Mukhopadhyay, M., Teufel, A., Yamashita, T., Agulnick, A. D., Chen, L., Downs, K. M., Schindler, A., Grinberg, A., Huang, S. P., Dorward, D. et al. (2003). Functional ablation of the mouse Ldb1 gene results in severe patterning defects during gastrulation. *Development* **130**, 495-505.

Nakano, T., Murata, T., Matsuo, I. and Aizawa, S. (2000). OTX2 directly interacts with LIM1 and HNF-3β. *Biochem. Biophys. Res. Commun.* **267**, 64-70.

Nieto, M. A., Bradley, L. C. and Wilkinson, D. G. (1991). Conserved segmental expression of Krox-20 in the vertebrate hindbrain and its relationship to lineage restriction. *Development Suppl.* **2**, 59-62.

Niwa, H., Yamamura, K. and Miyazaki, J. (1991). Efficient selection for high-expression transfectants with a novel eukaryotic vector. *Gene* **108**, 193-199.

Okazaki, Y., Furuno, M., Kasukawa, T., Adachi, J., Bono, H., Kondo, S., Nikaido, I., Osato, N., Saito, R., Suzuki, H. et al. (2002). Analysis of the mouse transcriptome based on functional annotation of 60,770 full-length cDNAs. *Nature* **420**, 563-573.

Oliver, G., Mailhos, A., Wehr, R., Copeland, N. G., Jenkins, N. A. and Gruss, P. (1995). Six3, a murine homologue of the sine oculis gene, demarcates the most anterior border of the developing neural plate and is expressed during eye development. *Development* **121**, 4045-4055.

Parr, B. A., Shea, M. J., Vassileva, G. and McMahon, A. P. (1993). Mouse Wnt genes exhibit discrete domains of expression in the early embryonic CNS and limb buds. *Development* **119**, 247-261.

Pramatarova, A., Goto, J., Nanba, E., Nakashima, K., Takahashi, K., Takagi, A., Kanazawa, I., Figlewicz, D. A. and Rouleau, G. A. (1994). A two basepair deletion in the SOD1 gene causes familial amyotrophic lateral sclerosis. *Hum. Mol. Genet.* **3**, 2061-2062.

Raval-Fernandes, S., Kickhoefer, V. A. and Rome, L. H. (1999). Cloning of a cDNA encoding a sequence-specific single-stranded-DNA-binding protein from Rattus norvegicus. *Gene* **237**, 201-207.

Rhinn, M., Dierich, A., Shawlot, W., Behringer, R. R., le Meur, M. and Ang, S. L. (1998). Sequential roles for *Otx2* in visceral endoderm and neuroectoderm for forebrain and midbrain induction and specification. *Development* **125**, 845-856.

Sasaki, H. and Hogan, B. L. (1994). HNF-3β as a regulator of floor plate development. *Cell* **76**, 103-115.

Sasaki, H., Nishizaki, Y., Hui, C., Nakafuku, M. and Kondoh, H. (1999). Regulation of Gli2 and Gli3 activities by an amino-terminal repression domain: implication of Gli2 and Gli3 as primary mediators of Shh signaling. *Development* **126**, 3915-3924.

Shawlot, W. and Behringer, R. R. (1995). Requirement for *Lim1* in head-organizer function. *Nature* **374**, 425-430.

Shawlot, W., Wakamiya, M., Kwan, K. M., Kania, A., Jessell, T. M. and Behringer, R. R. (1999). *Lim1* is required in both primitive streak-derived tissues and visceral endoderm for head formation in the mouse. *Development* **126**, 4925-4932.

Stoykova, A. and Gruss, P. (1994). Roles of *Pax*-genes in developing and adult brain as suggested by expression patterns. *J. Neurosci.* **14**, 1395-1412.

Suda, Y., Nakabayashi, J., Matsuo, I. and Aizawa, S. (1999). Functional equivalency between *Otx2* and *Otx1* in development of the rostral head. *Development* **126**, 743-757.

Tam, P. P. and Steiner, K. A. (1999). Anterior patterning by synergistic activity of the early gastrula organizer and the anterior germ layer tissues of the mouse embryo. *Development* **126**, 5171-5179.

Tam, P. P., Khoo, P. L., Wong, N., Tsang, T. E. and Behringer, R. R. (2004). Regionalization of cell fates and cell movement in the endoderm of the mouse gastrula and the impact of loss of *Lhx1(Lim1)* function. *Dev. Biol.* **274**, 171-187.

Thaler, J. P., Lee, S. K., Jurata, L. W., Gill, G. N. and Pfaff, S. L. (2002). LIM factor *Lhx3* contributes to the specification of motor neuron and interneuron identity through cell-type-specific protein-protein interactions. *Cell* **110**, 237-249.

Thomas, P. Q., Brown, A. and Beddington, R. S. (1998). Hex: a homeobox gene revealing peri-implantation asymmetry in the mouse embryo and an early transient marker of endothelial cell precursors. *Development* **125**, 85-94.

Tsang, T. E., Shawlot, W., Kinder, S. J., Kobayashi, A., Kwan, K. M., Schughart, K., Kania, A., Jessell, T. M., Behringer, R. R. and Tam, P. P. (2000). *Lim1* activity is required for intermediate mesoderm differentiation in the mouse embryo. *Dev. Biol.* **223**, 77-90.

Turner, D. L. and Weintraub, H. (1994). Expression of achaete-scute homolog 3 in *Xenopus* embryos converts ectodermal cells to a neural fate. *Genes Dev.* **8**, 1434-1447.

van Meyel, D. J., O'Keefe, D. D., Jurata, L. W., Thor, S., Gill, G. N. and Thomas, J. B. (1999). Chip and apterous physically interact to form a functional complex during Drosophila development. *Mol. Cell* **4**, 259-265.

van Meyel, D. J., Thomas, J. B. and Agulnick, A. D. (2003). Ssdp proteins bind to LIM-interacting co-factors and regulate the activity of LIM-homeodomain protein complexes in vivo. *Development* **130**, 1915-1925.

Vincent, S. D., Dunn, N. R., Hayashi, S., Norris, D. P. and Robertson, E. J. (2003). Cell fate decisions within the mouse organizer are governed by graded Nodal signals. *Genes Dev.* **17**, 1646-1662.

Wilkinson, D. C. (1992). Whole mount in situ hybridization of vertebrate embryos. *In Situ Hybridization: A Practical Approach* (ed. D. G. Wilkinson), pp. 75-84. Oxford, UK: Oxford University Press.